PAPER

www.rsc.org/loc

Thin-film polymer light emitting diodes as integrated excitation sources for microscale capillary electrophoresis

Joshua B. Edel,[a] Nigel P. Beard,[a] Oliver Hofmann,[c] John C. deMello,[a] Donal D. C. Bradley[b] and Andrew J. deMello*[a]

[a] *Department of Chemistry, Imperial College London, South Kensington, London, UK SW7 2AZ*
[b] *Department of Physics, Imperial College London, South Kensington, London, UK SW7 2AZ*
[c] *Molecular Vision Ltd., 90 Fetter Lane, London, UK EC4A 1JP*

Received 24th October 2003, Accepted 24th December 2003
First published as an Advance Article on the web 4th February 2004

We report the use of a thin-film polymer light emitting diode as an integrated excitation source for microfabricated capillary electrophoresis. The polyfluorene-based diode has a peak emission wavelength of 488 nm, an active area of 40 μm × 1000 μm and a thickness of ~2 mm. The simple layer-by-layer deposition procedures used to fabricate the polymer component allow facile integration with planar chip-based systems. To demonstrate the efficacy of the approach, the polyfluorene diode is used as an excitation source for the detection of fluorescent dyes separated on-chip by electrophoresis. Using a conventional confocal detection system the integrated pLED is successfully used to detect fluorescein and 5-carboxyfluorescein at concentrations as low as 10^{-6} M with a mass detection limit of 50 femtomoles. The drive voltages required to generate sufficient emission from the polymer diode device are as low as 3.7 V.

Introduction

Rapidly evolving frontiers in genomics, proteomics and medical diagnostics generate an ever-increasing demand for high throughput analytical information. The ability to extract the required information from a chemical or biological system almost always involves performing a number of distinct analytical operations. Ideal microfluidic systems will incorporate all such relevant steps including sample handling, sample pre-treatment, reaction, product separation, analyte detection, and product isolation.[1,2] While downsizing, system integration and parallelisation afford many performance gains including speed, analytical efficiency and throughput,[3–5] new problems are also encountered.

A significant challenge arising directly from the existence of small volumes within microfluidic systems is the ability to efficiently detect analyte molecules. For example, when performing capillary electrophoresis (CE) in microchannels, injection volumes typically range from 10^{-14} to 10^{-10} m^3. At a diagnostically relevant analyte concentration of 1 nanomolar, this results in between 10^3 and 10^7 detectable molecules. High-sensitivity detection is therefore a pre-requisite when performing analysis in microfluidic systems. To date, detection approaches for microfluidic analysis have generally focused on the use of optical techniques.[6] Optical measurements are well suited for most microfluidic systems due to the favourable optical characteristics of many substrate materials (including glasses, quartz, polymers, diamond and plastics) in the visible region of the electromagnetic spectrum. The most common chip based detection methods include laser-induced fluorescence (LIF),[7,8] UV–vis absorbance,[9,10] electrochemiluminescence,[11] refractive index variation[12,13] and thermal lens microscopy.[14] Although attractive for the detection of small molecules, absorbance measurements present a number of problems when used in microfluidic systems. This is primarily due to the difficulty in reconciling the small volumes representative of such systems with the need for a sufficiently long optical path length. While elegant solutions to the path length problem have been proposed,[15] sensitivity gains normally come at the expense of peak resolution when applied to separation devices. By far the most common optical detection technique for chip-based analysis is LIF which affords exceptional sensitivity and low mass detection limits. As few as 10^5 molecules are routinely detected, and recent developments in ultra-high sensitivity fluorescence detection have allowed single molecule detection to be performed within microchannel environments.[16]

'Off-chip' detection methods, based on external components, have been highly successful in the development of high-efficiency microfluidic systems for laboratory-based applications. However, the realization of portable microdevices for *in-the-field* or *point-of-care* applications[17,18] clearly necessitate the development of miniaturized and integrated detection systems. Considering potential compatibility problems in the fabrication of microfluidic and detection components, and the high degree of detection selectivity and sensitivity required,[19] this is not a trivial task. To date, relatively few examples of integrated optical components in microfluidic devices have been reported.[20] Examples have included the integration of microlenses/apertures,[21] and of silicon photodiodes and interference filters with glass microfluidic devices.[22,23] However, the majority of systems still rely on external light sources such as gas phase lasers,[21] solid state diode lasers[24] or inorganic light emitting diodes.[22,23,25]

Here we present a microchip based capillary electrophoresis (CE) device with an integrated, thin-film polymer light emitting diode (pLED) as an excitation source. A typical pLED comprises one or more layers of conjugated polymer sandwiched between two electrodes, of which at least one must be transparent (Fig. 1). The polymer emits light under electrical excitation (*via* radiative recombination of injected electrons and holes) and the devices may therefore be used as light sources. The emission colour is determined by the chemical structure of the polymers, and it may therefore be controlled using standard synthetic chemistry. In this manner, multiple pLEDs that span the full visible spectrum from blue to red may be fabricated. Many of the polymers are soluble, allowing for low cost deposition from solution (including inkjet printing). Owing to the simple layer-by-layer deposition procedures for the polymer components and the planar structure of analytical microchips, the pLEDs may be easily integrated into existing chip structures at marginal additional cost. The tunable optical properties, simple fabrication, small size and low cost of pLEDs[26–28] have already attracted considerable interest in display technology.[29,30] The presented work is aimed at extending the applications of pLEDs to microfluidic systems.

Experimental

Chip fabrication

CE microdevices were manufactured in-house and comprised a microchannel network etched into a planar glass substrate. Fabrication of the microdevices involved a three-step process:

DOI: 10.1039/b313503a

layout design and fabrication of a chromium mask, etching and preparation of the substrate surface, followed by thermal bonding of the substrate to a cover plate.

The channel pattern was designed using AutoCAD® and transferred onto a glass wafer pre-coated with a chromium layer and positive photoresist (Nanofilm, Westlake Village, CA, USA) using a direct-writing photolithographic system (DWL2.0, Heidelberg Instruments, Heidelberg, Germany). Exposed photoresist was removed with a 5 : 1 v/v-ratio mixture of water and developing agent (Microposit, Coventry, UK). This was followed by a chromium etching procedure using a Lodyne etchant (Microchem Systems, Coventry, UK). The exposed channel network was then etched with a buffered oxide etchant ($HF–NH_4F$) solution at ambient temperature yielding an etch rate of 0.1 ± 0.02 μm min^{-1}. Upon completion of the etching the substrate was cleaned by sequential sonication in methanol, $H_2SO_4–H_2O_2$ and ultra pure water, followed by drying in a stream of nitrogen.

To form an enclosed microfluidic structure, a cover plate was thermally bonded to the substrate by heating the assembly to 550 °C for 1 hour, 585 °C for 8 hours and 555 °C for 1 hour. The complete device was then allowed to cool down to ambient temperature over a period of 8 hours. The cover plate was subsequently polished down to a thickness of ~150 μm. Optical polishing of the cover plate was required to accommodate the small working distance of the microscope objective used for fluorescence detection. Finally fluidic access holes were drilled into the thin cover plate using an electrochemical discharge method.[31] A 0.5 mm diameter platinum wire was used as the drilling needle, and a constant spark was generated by applying 150 V to the needle tip submerged in an 8 M NaOH solution.

pLED fabrication

The pLEDs used in the current study were based on blue light emitting polyfluorenes, representative of present state of the art performance. The device structures typically comprised a patterned indium tin oxide [ITO] coated glass substrate onto which poly(3,4-ethylenedioxythiophene)/polystyrene sulfonate [PEDOT/PSS] was coated from aqueous solution (Baytron P®, HC Stark) to form a hole-injecting, anode layer. The active polyfluorene emission layer (homopolymer, copolymer or blend)[32] was then deposited from organic solvent to a layer thickness of 50–100 nm by spin coating. The metal, electron-injecting, cathode was thermally evaporated on top, with typically a few nm of LiF deposited first and capped with a few hundred nm of Al. The finished structure was encapsulated under inert gas in a glove box by sealing a metal can or glass plate on top (using an epoxy resin). The structure is "bottom emitting" *i.e.* the light emerges from the polyfluorene layer through the PEDOT/PSS, ITO and glass. Owing to the simple layer-by-layer deposition procedures for the polymer components and the planar structure of analytical microchips, the pLEDs may be easily integrated into existing chip structures at marginal additional cost.

The emission bandwidth for pLEDs is relatively broad, due both to the vibronic progression associated with the π*–π electronic transition (characteristic vibrational mode energies of 150–200 meV) and inhomogeneous broadening. For the devices for which results are reported here the emission maximum occurs at 488 nm and the bandwidth (FWHM) is some 85 nm, extending from 439 nm to 524 nm. This device was specifically chosen due to the appreciable overlap of its emission spectrum with the absorption spectra of the xanthene dyes used in the current studies (fluorescein and carboxyfluorescein). Integration of the pLED with the planar CE microdevice was simply achieved by aligning and attaching the bottom, glass output face of the pLED to the underside of the planar chip using a thin layer of optically transparent glue (Araldite Instant Clear). The pLEDs had an active area of 40 μm × 1000 μm, and a thickness of 2 mm. This resulted in an overall microdevice thickness of less than 3.5 mm.

Separation conditions

The layout of the microfabricated CE device is shown schematically in Fig. 1. The device comprises an injection channel and a variable length separation channel. Microchannels have an average width of 50 μm and are 40 μm deep. The distances from the injection point to the sample inlet (reservoir 1), sample outlet (reservoir 3), buffer inlet (reservoir 2), and buffer outlets (reservoirs 4,5,6) are 18.2 mm, 18.2 mm, 6.6 mm and 26.0/35.5/27.2 mm, respectively. For the reported experiments reservoirs 4 and 5 were not used. Prior to experimentation microchannels were pretreated sequentially with 1 M sodium hydroxide, deionized water (18 MΩ) and tris-borate–EDTA buffer. This process ensured generation of a sufficiently high electroosmotic flow during electrophoretic separation. The microdevice was operated in one of two modes, *sample loading* or *separation* mode. An 8-channel power supply generating up to 3000 V was used to supply the drive voltages for electrophoresis. Platinum wire electrodes served as electrical contacts between the power supply and fluidic reservoirs. First, the injection channel was filled by applying vacuum to the sample outlet (3). The sample volume in the microchannel intersection (~100 pL) was then injected into the separation channel by application of an electric field between the buffer inlet (2) and outlet reservoir (6). For characterization of the pLED response and for determination of the detection limit a second injection mode was used. Again the injection channel was filled by applying vacuum to the sample outlet (3). This time filling of the separation channel *via* capillary force was allowed to proceed until almost the entire channel was filled. The corresponding plug of ~50 nL was

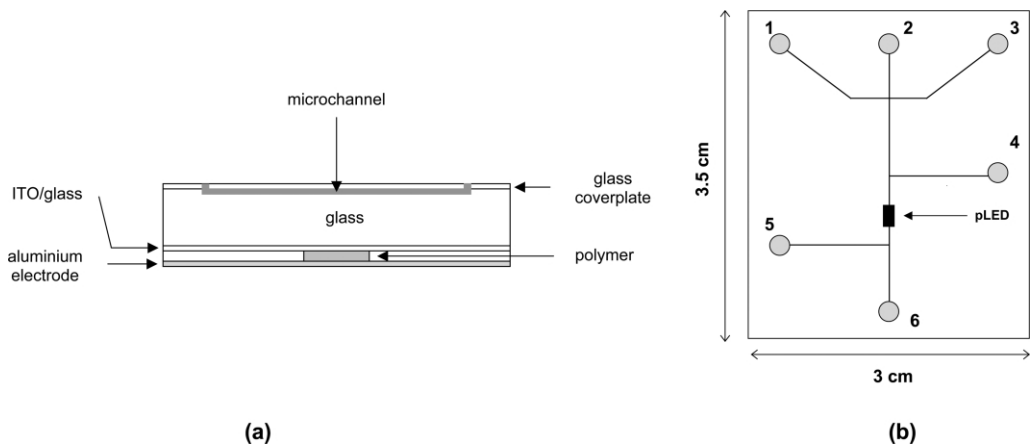

Fig. 1 (a) Side view (not to scale) of pLED integrated with a planar glass CE microdevice. (b) Layout of the CE microdevice, comprising an injection channel and a variable length separation channel: 1 sample inlet, 2 buffer inlet, 3 sample outlet, 4–6 buffer outlets (4 & 5 unused). Microchannels are 50 μm wide and 40 μm deep. The pLED (active area: 40 μm × 1000 μm) is positioned below the separation channel between outlets 4 & 5.

subsequently motivated past the detector by applying vacuum to buffer outlet (6).

Materials

10 mM stock solutions of fluorescein (Sigma-Aldrich, Gillingham, UK) and 5-carboxyfluorescein (Molecular Probes, Leider, The Netherlands) were prepared in TBE buffer (tris-borate–EDTA). The TBE buffer was prepared by dissolving a solid TBE mixture (Fluka Chemicals, Gillingham, UK) in 18 MO deionized water to a final concentration of 8.9 mM tris(methoxy)aminomethane, 8.9 mM boric acid and 0.2 mM of ethylenediaminetetraacetic acid. For all experiments freshly prepared solutions were used.

Detection system

Electrophoretic separations of fluorescein and 5-carboxyfluorescein were monitored using either a conventional 50 W mercury lamp or the integrated pLED as an excitation source. For mercury lamp excitation, detection was performed using an inverted fluorescence microscope (DMIL; Leica, Milton Keynes, UK). In an epi-illumination configuration, excitation light was passed through an excitation filter (BP 450–490 nm), reflected by a dichroic mirror (RKP 510) and focused onto the microchip *via* the microscope objective (10×, 0.42 N.A.) (Newport, Irvine, CA, USA). Fluorescence emitted from the microchip was collected with the same objective and passed through the dichroic mirror, a suppression filter (BP 515–560 nm), and an adjustable pinhole set to 20 μm × 60 μm. A photomultiplier tube (MEA153; Seefelder Messtechnik, Germany) operated in the current mode was employed to detect any fluorescence photons. Data were acquired at 20 Hz with a Picolog data acquisition card (Pico Technology, Hardwick, Cambridge, UK) and processed with Origin software (Microcal Software, Northampton, USA).

For pLED excitation, detection of bulk solutions was performed using an Ocean Optics S2000 spectrometer interfaced with a 400 μm-diameter optical fibre (Ocean Optics, Netherlands). For capillary electrophoresis, fluorescence originating from sample in the separation channel was collected using a 100×/1.3 N.A., oil immersion objective (Carl Zeiss, Welwyn Garden City, UK). An emission filter (515EFLP; Omega Optical) was employed to reduce transmission of residual excitation light. A plano-convex lens (+50.2 F; Newport) focused the fluorescence onto a precision pinhole (5–200 μm; Melles Griot) positioned immediately in front of the detector. The pinhole coincided with the confocal plane of the microscope objective. The detector was a silicon avalanche photodiode (SPCM-AQR-141; EG&G Canada, Vaudreuil, Quebec, Canada) with an average dark count rate below 100 Hz. The pinhole and detector were mounted on an XYZ translation stage to facilitate positioning relative to the incoming radiation from the microchip. The electronic signal from the detector was coupled to a lock-in amplifier and then recorded at an acquisition rate of 10 Hz using an ADC-40 Picolog data acquisition card (Pico Technology, St. Neots, UK).

Results and discussion

Initial experiments utilized the fabricated pLED as an excitation source for bulk solution emission spectroscopy. The pLED was mounted on the underside of a microscope slide (BDH Merck, Poole, UK) containing a 3 mm-deep sample well. Fig. 2(a) shows the electroluminescence spectrum of the pLED and a normalised absorption spectrum of a 10 μM fluorescein solution. It is observed that the pLED emission characteristics (λ_{max} = 488 nm) are well matched to the absorption band of fluorescein in solution (λ_{max} = 490 nm). Fig. 2(b) shows an emission spectrum for a 10 μM fluorescein solution excited by the pLED. The high-energy emission peak visible between 420 and 500 nm corresponds to the emission of the pLED, with low energy emission above 480 nm describing the singlet-state emission of fluorescein. The relative intensity of the vibronic bands at 450 and 488 nm is different to that observed in Fig. 2(a). This is due to the appreciable overlap of the electroluminescence spectrum of the pLED and the absorption spectrum of fluorescein mediating significant self-absorption.[33]

Current density–voltage and signal–voltage curves for the pLED integrated with the microfabricated CE device are shown in Fig. 3. It can be seen that the turn-on voltage (onset of current) occurs at approximately 2.7 V (0.05 A m^{-2}). The signal–voltage curve characterizes the response of the CE microdevice detection system. A minimum pLED drive voltage of approximately 3.7 V (corresponds to a minimum current density of 2 A m^{-2}) was required for the detection system to register photons. The maximum voltage applied to the pLED was 8 V with a current density of 200 A m^{-2}.

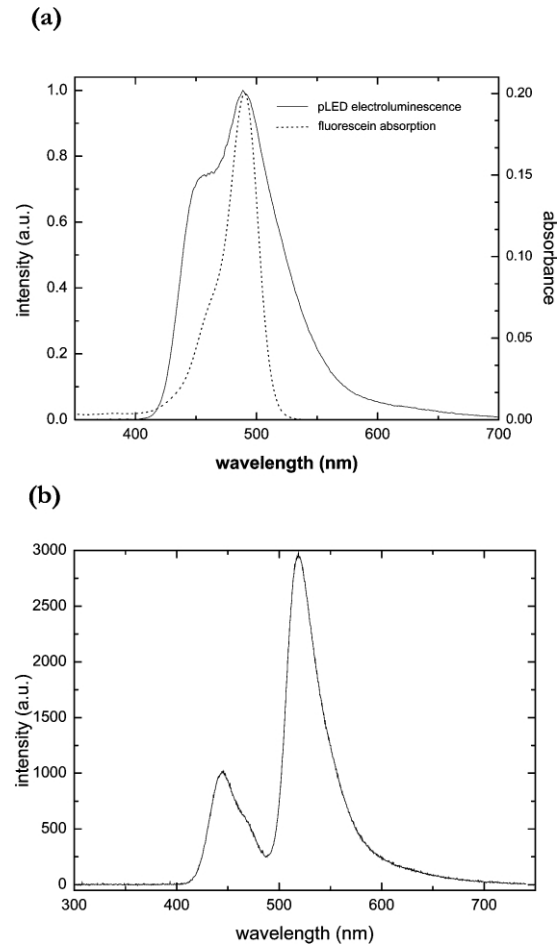

Fig. 2 (a) Absorption and normalised electroluminescence emission spectra of 10 μM fluorescein in tris-borate–EDTA buffer and the polyfluorene pLED, respectively. (b) Fluorescence emission spectrum of 10 μM fluorescein in tris-borate–EDTA buffer; pLED drive voltage = 8 V.

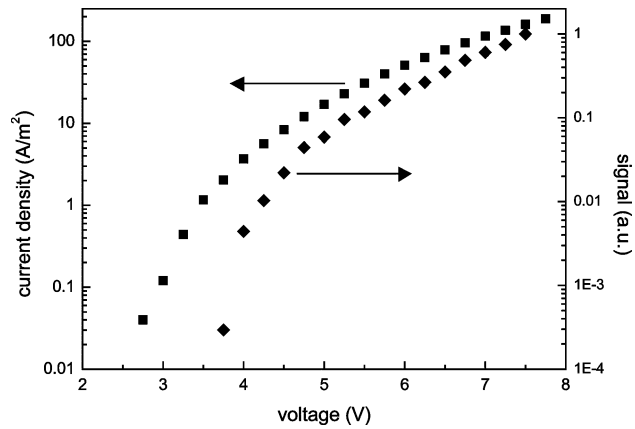

Fig. 3 Variation of current density and recorded signal as a function of pLED applied bias.

The difference between the onset of current and the onset of a recorded signal can be attributed to light scattering processes. Emitted photons from the pLED must travel through the CE glass microdevice (total thickness ~1.3 mm) before reaching the collection objective.

A 10 mM fluorescein solution was used to determine the effect of the pLED drive voltage on signal to noise in the CE microdevices. Fig. 4 shows detected fluorescence emission from fluorescein plugs (~50 nL) being hydrodynamically motivated through the separation channel at various pLED drive voltages. For higher pLED voltages the signal-to-noise (S/N) ratios were observed to be significantly higher than for lower voltages. A maximum S/N of 840 was obtained at 7 V. It should be noted that since the lock-in amplifier time constant was 3 s for these measurements peak resolution was compromised. While a higher S/N ratio could be achieved by increasing the time constant of the lock-in amplifier further, this is clearly unsuitable for chip-based applications where separation times are typically below 10 s. Consequently, for all electrophoretic separations time constants of 100 ms were used.

The ratio of total signal to pLED emission as a function of voltage is shown in Fig. 5. As stated previously the total measured signal is a combination of the output of the pLED and analyte fluorescence. At low drive voltages (4–5.5 V) an approximate linear increase in the ratio of total signal to pLED emission is observed. The ratio of total signal to pLED emission reaches a limiting value of approximately 8.5 for drive voltages above 7 V. It is interesting to note that the variation in S/N does not follow the same trend; with a continuous increase in S/N as drive voltage is increased. We believe this trend is due to the significantly lower noise levels encountered at higher pLED drive voltages.

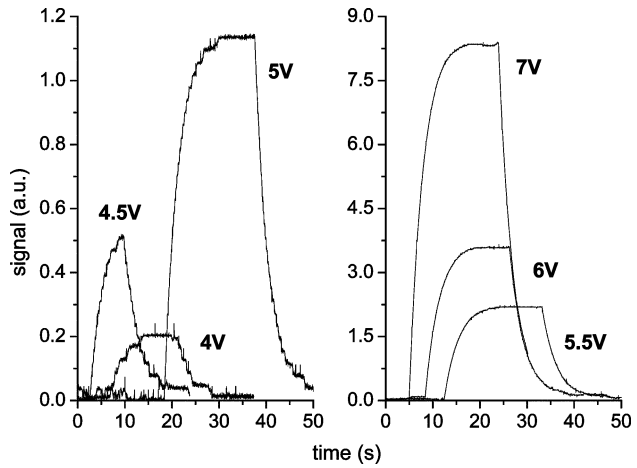

Fig. 4 Detection of ~50 nL plugs of fluorescein (10 mM) moving through a microchannel (50 μm wide, 40 μm deep); pLED drive voltage = 4–7 V; pinhole = 50 μm. Data were recorded using a time constant of 3 s.

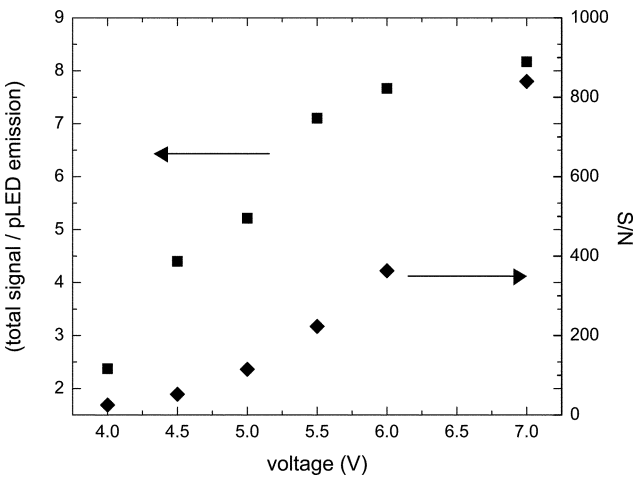

Fig. 5 Variation of total signal to pLED emission ratio and signal-to-noise ratio as a function of pLED applied bias. Conditions as in Fig. 4.

These initial calibration studies clearly indicate that for sensitive detection, high pLED drive voltages are beneficial. However, high voltages applied over extended time periods can severely compromise the output stability as well as device lifetime.[27] Consequently, for analytical applications a compromise between detection sensitivity and pLED lifetime has to be found. In the current studies it was decided to use a pLED drive voltage of 6 V or lower for all electrophoretic studies.

Initial chip-based experiments focused on the influence of the confocal pinhole on signal intensities. Fig. 6 illustrates repeat injections of 10 mM fluorescein using pinhole sizes of 25, 50, and 200 μm and a pLED drive voltage of 6 V. Increasing the pinhole size resulted in an improved signal to noise but no significant effect on peak resolution. This indicates that the separated zones in the microchannel were larger than the maximum pinhole size employed. Furthermore, the repetitive injection results demonstrate that the pLED has good stability at the second to minute time scale.

Electrophoretic analyses of a mixture of fluorescein (5 mM) and 5-carboxyfluorescein (5 mM) using the pLED or a mercury lamp as an excitation source are shown in Fig. 7. Electrokinetic injection of

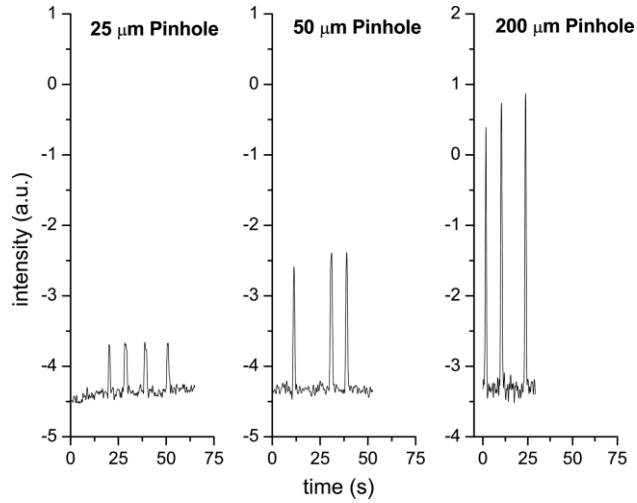

Fig. 6 Repeat 100 pL injections of 10 mM fluorescein solution into the separation microchannel (50 μm wide, 40 μm deep). pLED drive voltage = 6 V, separation voltage = 3000 V, pinhole = 25, 50 or 200 μm. Data were recorded using a time constant of 100 ms.

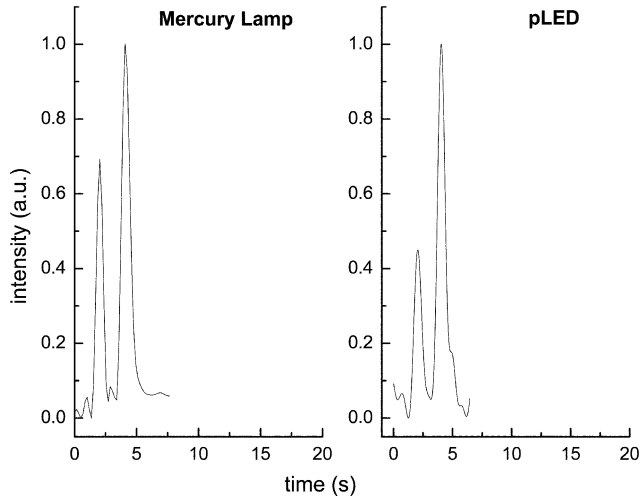

Fig. 7 Electrophoretic separation of 100 pL plugs of fluorescein and 5-carboxyfluorescein (both 5 mM). Sample excitation effected using either the integrated pLED or mercury lamp. pLED drive voltage = 6 V, separation voltage = 3000 V, pinhole = 50 μm. Data were recorded using a time constant of 100 ms.

a 100 pL sample plug and separation were both performed using an applied voltage of 3000 V. For pLED excitation a constant drive voltage of 6 V and a pinhole size of 50 μm were employed. The detection window for the mercury lamp excitation was set to be approximately the same size. Both separations are complete within 5 seconds yielding identical migration times for each component (2.05 ± 0.05 s for fluorescein and 4.05 ± 0.05 s for 5-carboxyfluorescein). The observed peak intensities for both excitation/detection geometries are broadly similar.

Fig. 8 shows a calibration curve for fluorescein. For pLED excitation a drive voltage of 5.5 V and a 50 μm pinhole were used. The detection limits for both the lamp and pLED detection systems were approximately 1 μM. Given an estimated injection plug volume of 50 nL this corresponds to a mass detection limit of 50 femtomoles. It can be seen that the slopes of both calibration curves are broadly similar. Improved detection limits for the pLED based system could be gained through the use of higher pLED drive voltages and larger pinholes.

Conclusions and outlook

An integrated polyfluorene pLED excitation source was characterized and applied to the detection of fluorescein and 5-carboxyfluorescein in a microfabricated CE device. The pLED emission was measured to be in the range of 400–600 nm (blue–green), coinciding with the excitation maxima of both employed fluorophores. A minimum pLED drive voltage of 3.7 V was required for light emission. Higher light intensities were achieved by increasing the drive voltage. Highest S/N ratios were obtained for drive voltages in excess of 7 V. However, since the stability of the light output and the lifetime of the pLED are compromised by high drive voltages, 6 V was used for analytical applications. With the pLED excitation source attached to a microfabricated CE device, separations of fluorescein and 5-carboxyfluorescein could easily be detected. A mass detection limit for fluorescein was determined to be 50 femtomoles for a pinhole size of 50 μm. Similar detection limits were obtained with a conventional mercury lamp excitation source.

Whilst higher excitation intensities and lower detection limits are still afforded by laser light sources, the small size and low cost of pLEDs have obvious benefits for portable *in-the-field* and *point-of-care* devices. Future research efforts are focused on increasing the light output without compromising the lifetime of pLEDs. Such miniaturized optical light sources, when combined with thin-film polymer photodetectors, should yield powerful integrated polymer detection systems for a wide range of applications. Over the next ten years we envisage polymer based detection arrays becoming a key component of multi-analyte microfluidic systems for the point-of-care market.

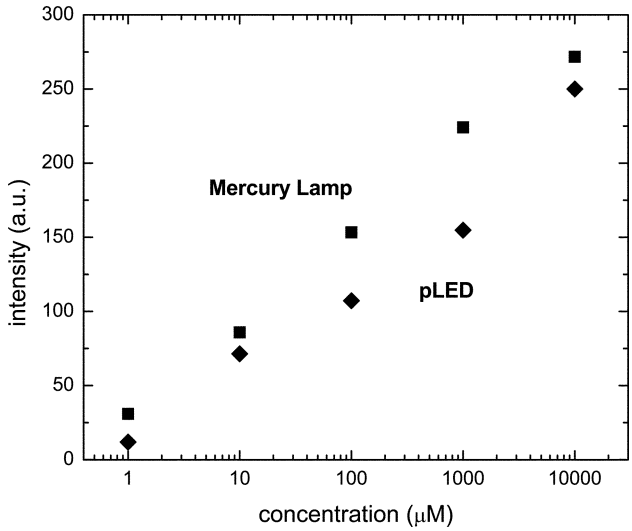

Fig. 8 Variation of intensity as a function of analyte concentration for 50 nL plugs. For pLED excitation, drive voltage = 5.5 V, pinhole for all measurements = 50 μm. Data were recorded using a time constant of 3 s.

Acknowledgement

The Imperial College authors thank the UK Engineering and Physical Sciences Research Council (GR/R58949) and Molecular Vision Ltd for funding this work. We also thank Cambridge Display Technology Ltd for providing test pLEDs. Molecular Vision Ltd acknowledges support from the UK Biotechnology and Biological Sciences Research Council through its Small Business Research Initiative (grant 147/SBRI 19689). J.B.E. is a recipient of an Overseas Research Scholarship from the UK Government.

References

1 D. R. Reyes, D. Iossifidis, P. A. Auroux and A. Manz, *Anal. Chem.*, 2002, **74**, 2623.
2 P. A. Auroux, D. Iossifidis, D. R. Reyes and A. Manz, *Anal. Chem.*, 2002, **74**, 2637.
3 G. H. W. Sanders and A. Manz, *TrAC–Trends Anal. Chem.*, 2000, **19**, 364.
4 S. C. Jakeway, A. J. de Mello and E. L. Russell, *Fresenius' J. Anal. Chem.*, 2000, **366**, 525.
5 E. Verpoorte, *Electrophoresis*, 2002, **23**, 677.
6 M. A. Schwarz and P. C. Hauser, *Lab Chip*, 2001, **1**, 1.
7 D. J. Harrison, K. Fluri, K. Seiler, Z. H. Fan, C. S. Effenhauser and A. Manz, *Science*, 1993, **261**, 895.
8 B. B. Haab and R. A. Mathies, *Anal. Chem.*, 1999, **71**, 5137.
9 E. Verpoorte, A. Manz, H. Ludi, A. E. Bruno, F. Maystre, B. Krattiger, H. M. Widmer, B. H. Vanderschoot and N. F. Derooij, *Sens. Actuators, B*, 1992, **6**, 66.
10 Z. H. Liang, N. Chiem, G. Ocvirk, T. Tang, K. Fluri and D. J. Harrison, *Anal. Chem.*, 1996, **68**, 1040.
11 A. Arora, J. C. T. Eijkel, W. E. Morf and A. Manz, *Anal. Chem.*, 2001, **73**, 3282.
12 N. Burggraf, B. Krattiger, A. J. de Mello, N. F. de Rooij and A. Manz, *Analyst*, 1998, **123**, 1443.
13 K. Swinney, D. Markov and D. J. Bornhop, *Anal. Chem.*, 2000, **72**, 2690.
14 K. Sato, H. Kawanishi, M. Tokeshi, T. Kitamori and T. Sawada, *Anal. Sci.*, 1999, **15**, 525.
15 H. Salimi-Moosavi, Y. T. Jiang, L. Lester, G. McKinnon and D. J. Harrison, *Electrophoresis*, 2000, **21**, 1291.
16 A. J. de Mello, *Lab Chip*, 2003, **3**, 29N.
17 C. P. Price, *Disease Manage. Health Outcomes*, 2002, **10**, 749.
18 A. J. Tudos, G. A. J. Besselink and R. B. M. Schasfoort, *Lab Chip*, 2001, **1**, 83.
19 B. D. Malhotra and A. Chaubey, *Sens. Actuators, B*, 2003, **91**, 117.
20 E. Verpoorte, *Lab Chip*, 2003, **3**, 42N.
21 J. C. Roulet, R. Volkel, H. P. Herzig, E. Verpoorte, N. F. de Rooij and R. Dandliker, *Anal. Chem.*, 2002, **74**, 3400.
22 M. A. Burns, B. N. Johnson, S. N. Brahmasandra, K. Handique, J. R. Webster, M. Krishnan, T. S. Sammarco, P. M. Man, D. Jones and D. Heldsinger, *Science*, 1998, **282**, 484.
23 J. R. Webster, M. A. Burns, D. T. Burke and C. H. Mastrangelo, *Anal. Chem.*, 2001, **73**, 1622.
24 G. F. Jiang, S. Attiya, G. Ocvirk, W. E. Lee and D. J. Harrison, *Biosens. Bioelectron.*, 2000, **14**, 861.
25 Q. Lu and G. E. Collins, *Analyst*, 2001, **126**, 429.
26 J. H. Burroughes, D. D. C. Bradley, A. R. Brown, R. N. Marks, K. Mackay, R. H. Friend, P. L. Burns and A. B. Holmes, *Nature*, 1990, **347**, 539.
27 R. H. Friend, R. W. Gymer, A. B. Holmes, J. H. Burroughes, R. N. Marks, C. Taliani, D. D. C. Bradley, D. A. Dos Santos, J. L. Bredas and M. Logdlund, *Nature*, 1999, **397**, 121.
28 D. Braun, *Mater. Today*, 2002, **June**, 32.
29 K. Ziemelis, *Nature*, 1999, **399**, 408.
30 W. E. Howard and O. F. Prache, *IBM J. Res. Dev.*, 2001, **45**, 115.
31 S. Shoji and M. Esashi, in *Technical Digest of the 9th Sensor Symposium* p. 27, Japan, 1990.
32 www.cdtltd.co.uk.
33 S. Dhami, A. J. deMello, G. Rumbles, S. M. Bishop, D. Phillips and A. Beeby, *Photochem. Photobiol.*, 1995, **61**, 341.